

Disorder and Interactions in 1D Systems

Jonathan M Carter and Angus MacKinnon

*Blackett Laboratory, Imperial College London, South Kensington Campus, London SW7 2AZ, UK**

(Dated: February 8, 2020)

We present a new numerical approach to the study of disorder and interactions in quasi-1D systems which combines aspects of the transfer matrix method and the density matrix renormalization group which have been successfully applied to disorder and interacting problems respectively. The method is applied to spinless fermions in 1D and the existence of a conducting state is demonstrated in the presence of attractive interactions.

PACS numbers: 71.30.+h, 71.55Jv, 72.15Rn

I. INTRODUCTION

It is well established that in the presence of disorder electron wavefunctions can become localized. Considerable numerical work has been carried out for non-interacting systems with results reaching a reasonable consensus: theory and experiment are in general qualitative agreement. However, in 3D the calculated value of the universal critical exponent is markedly larger than the empirically measured value¹. This seems to suggest that an essential factor is missing from calculations: the obvious candidate is the electron-electron interaction. Furthermore, some have claimed to observe a Metal-Insulator transition in 2D contrary to the widely accepted scaling theory of Anderson localization². This is often accredited to the effect of interactions. Hence during the last 10 years attention has been switching to this more difficult case. The central problem is that the model becomes a many-body system and so the Hilbert space grows quickly with system size. This renders an exact numerical calculation far beyond computational capabilities. Nevertheless, several studies have been accomplished, these suggest inclusion of interactions may yield non-trivial behavior.

Shepelyansky³ performed calculations on two interacting particles. In 1D, interactions caused a large enhancement of localization length. Other work showed that in 2D the effect is possibly stronger leading to delocalization⁴. However, some caution is required as the method fails to reproduce known non-interacting results when interactions are switched off.

The most successful method for treating the finite density problem is the Density Matrix Renormalization Group (DMRG) approach^{5,6}. This works by performing a direct diagonalization but reducing the Hilbert space by systematically discarding basis states that do not contribute significantly to the ground state. Applying this method to the Anderson interacting model (defined in equation 1), a delocalized regime was found for attractive interactions⁷. In more recent papers by the same authors, it was noted that interesting physics is washed out in the averaging process. Charge reorganizations can be seen as electrons on a chain shift from the Mott insulator limit (strong interactions) to the Anderson insula-

tor limit (strong disorder)⁸. Extensions of DMRG to 2D have encountered difficulties.

We have developed a new method incorporating some of the ideas of DMRG and the transfer matrix method successfully used in the non-interacting case^{9,10}. Section II describes the method and section III discusses the application to a model of spinless fermions.

II. THE NEW METHOD

Like DMRG our approach is based on a tight-binding method and has a similar potential usefulness. It can be readily applied to describe any 1D or quasi-1D system, provided interactions are nearest-neighbor.

A. The Hamiltonian

As this is a many-body problem it is natural to work within the second quantization formalism of quantum mechanics. This allows the Hamiltonian to be written in terms of particle creation \hat{c}_i^\dagger and annihilation \hat{c}_i operators for site i :

$$\hat{H} = \sum_i \varepsilon_i \hat{c}_i^\dagger \hat{c}_i + V \sum_i (\hat{c}_i^\dagger \hat{c}_{i+1} + \hat{c}_{i+1}^\dagger \hat{c}_i) + U \sum_i (\hat{c}_i^\dagger \hat{c}_i)(\hat{c}_{i+1}^\dagger \hat{c}_{i+1}) - \mu \sum_i \hat{c}_i^\dagger \hat{c}_i. \quad (1)$$

The first two terms constitute the standard Anderson model¹¹ used widely in the study of disorder induced localization. The additional U term represents the nearest-neighbor interaction. If neighboring sites are occupied then the two particles experience a repulsive force (as for electrons) or possibly attractive force of strength U . Setting $U = 0$ reverts the system to the many independent-body situation (i.e. the non-interacting case).

The final term represents the chemical potential μ . It is necessary as this method works within the grand canonical scheme in which a range of particle numbers will be considered. The value of the parameter μ corresponds to the energy required to add a particle to the system, and thus controls the particle density of the system ground state. As with most numerical studies of Anderson localization zero temperature will be assumed.

B. The Recursive Method

Our method tackles the problem of the exponentially growing Hilbert space by reducing the number of basis states, restricting the focus to the ground state. This works in conjunction with a recursive procedure that extends the chain by successively adding new sites. Open boundary conditions must be used.

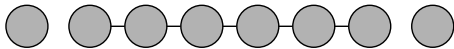


FIG. 1: The recursive procedure adds new sites to both ends of a 1D chain at each iteration.

For each iteration:

- A site is added to each end of the chain (fig. 1) and basis states are constructed. At first sight it may appear simpler to add a new site to one end only. However, it turns out that for the purposes of measuring the degree of localization it is much more natural to add sites to both ends of the chain in the same iteration (section II C).
- For each particle number with remaining basis states a Hamiltonian matrix is found. After the matrix elements have been calculated, the Hamiltonian is solved and the desired quantities are extracted.
- Finally, a proportion of the resulting eigenstates are thrown away according to some criterion. The remaining states are used to form the basis at the next iteration - a chain with two more sites.

There is no fundamental reason why this process cannot be repeated to very large chain lengths. The following sections detail the mathematics of this procedure.

1. Expressing the Basis States

For a one-dimensional chain, with L sites and one electron per site, there are 2^L basis states. In order to reduce the Hilbert space, this new method relies on the fact that it is possible to express the states for a chain of length L in terms of the energy eigenstates $|\Phi^{L-2}\rangle$ of the chain of length $L-2$ (i.e. the same chain without the two end sites). Formally, the L site Hilbert space is a product of the Hilbert space for the $L-2$ site chain with the vector space associated with the two new sites.

The eigenstates $|\Phi^{L-2}\rangle$ can be used as an orthogonal basis for the inner Hilbert space because they are eigenvectors of the previous iteration Hamiltonian such that

$$\hat{H}^{L-2}|\Phi_i^{L-2}\rangle = E_i|\Phi_i^{L-2}\rangle. \quad (2)$$

The outer Hilbert space, associated with the two new sites, is spanned by four basis states. This is readily seen by considering particle number occupancy representation: $|0\cdots 0\rangle$, $|1\cdots 0\rangle$, $|0\cdots 1\rangle$ and $|1\cdots 1\rangle$. Thus for every eigenstate $|\Phi_i^{L-2}\rangle$ of the $L-2$ site chain, there are four corresponding basis states for the L chain: $|0\Phi_i^{L-2}0\rangle$, $|1\Phi_i^{L-2}0\rangle$, $|0\Phi_i^{L-2}1\rangle$ and $|1\Phi_i^{L-2}1\rangle$.

Consequently, a general state for the L chain with N electrons, $|\Psi_n^{L,N}\rangle$, may be written as a linear combination of basis states in the following manner:

$$\begin{aligned} |\Psi_n^{L,N}\rangle = & \sum_i a_{ni} |0\Phi_i^{L-2,N}0\rangle \\ & + \sum_j \left\{ b_{nj} |1\Phi_j^{L-2,N-1}0\rangle + c_{nj} |0\Phi_j^{L-2,N-1}1\rangle \right\} \\ & + \sum_k d_{nk} |1\Phi_k^{L-2,N-2}1\rangle. \end{aligned} \quad (3)$$

In fact, as this equation indicates, it is only necessary to consider the subset of $|\Phi^{L-2}\rangle$ states which, when combined with two new end sites, have a total of N electrons. The reason is that particle number is a good quantum number for this Hamiltonian.

2. Calculating the Hamiltonian Matrix

Thus basis states can be grouped according to particle number and a separate Hamiltonian can be calculated for each. This can only be accomplished by first expanding each of the four types of basis states for N particles and $L-2$ sites back a further generation, in terms of the previous iteration $|\Phi^{L-4}\rangle$:

$$\begin{aligned} |m\Phi_i^N n\rangle = & \sum_p a_{ip}^{mn} |m0\Phi_p^{N-2}0n\rangle \\ & + \sum_q b_{iq}^{nm} |m1\Phi_q^{N-1}0n\rangle \\ & + \sum_r c_{ir}^{mn} |m0\Phi_r^{N-1}1n\rangle \\ & + \sum_s d_{is}^{mn} |m1\Phi_s^{N-2}1n\rangle \end{aligned} \quad (4)$$

where $m, n = 0, 1$ and the $L-4$ superscripts have been dropped for the sake of clarity. It is now possible to cast the Hamiltonian in a corresponding form. This involves some tedious algebra. However, bearing in mind that the states for different N are orthogonal as are the sets of eigenstates Φ_p^{L-2} and Φ_q^{L-4} of the Hamiltonian at the 2 previous iterations, the final Hamiltonian may be written as the following 4×4 block form:

	$ 0\Phi_i^N 0\rangle$	$ 1\Phi_j^{N-1} 0\rangle$	$ 0\Phi_j^{N-1} 1\rangle$	$ 1\Phi_k^{N-2} 1\rangle$
$\langle 0\Phi_{i'}^N 0 $	$E_i \delta_{i'i}$	$V \sum_q b_{i'q}^{00} a_{jq}^{10}$ $+V \sum_r d_{i'r}^{00} c_{jr}^{10}$	$V \sum_q c_{i'q}^{00} a_{jq}^{01}$ $+V \sum_r d_{i'r}^{00} b_{jr}^{01}$	0
$\langle 1\Phi_{j'}^{N-1} 0 $	$V \sum_q a_{j'q}^{10} b_{iq}^{00}$ $+V \sum_r c_{j'r}^{10} d_{ir}^{00}$	$(E_j + \varepsilon_1 - \mu) \delta_{j'j}$ $+U \sum_r b_{j'r}^{10} b_{jr}^{10}$ $+U \sum_s d_{j's}^{10} d_{js}^{10}$	0	$V \sum_r c_{j'r}^{10} a_{kr}^{11}$ $+V \sum_s d_{j's}^{10} b_{ks}^{11}$
$\langle 0\Phi_{j'}^{N-1} 1 $	$V \sum_q a_{j'q}^{01} c_{iq}^{00}$ $+V \sum_r b_{j'r}^{01} d_{ir}^{00}$	0	$(E_j + \varepsilon_L - \mu) \delta_{j'j}$ $+U \sum_r c_{j'r}^{01} c_{jr}^{01}$ $+U \sum_s d_{j's}^{01} d_{js}^{01}$	$V \sum_r b_{j'r}^{01} a_{kr}^{11}$ $+V \sum_s d_{j's}^{01} c_{ks}^{11}$
$\langle 1\Phi_{k'}^{N-2} 1 $	0	$V \sum_r a_{k'r}^{11} c_{jr}^{10}$ $+V \sum_s b_{k's}^{11} d_{js}^{10}$	$V \sum_r a_{k'r}^{11} b_{jr}^{01}$ $+V \sum_s c_{k's}^{11} d_{js}^{01}$	$(E_k + \varepsilon_1 + \varepsilon_L - 2\mu) \delta_{k'k}$ $+U \sum_s b_{k's}^{11} b_{ks}^{11} + U \sum_s c_{k's}^{11} c_{ks}^{11}$ $+2U \sum_t d_{k't}^{11} d_{kt}^{11}$

For each particle number with a set of basis states, this block matrix can be used to generate the elements of the full matrix. A ground state can be calculated for each of these particle numbers. The ground state lowest in energy is the system ground state (this is how μ controls the ground state particle density).

3. Reducing the Number of Basis States

The purpose of reformulating the basis states and in turn the Hamiltonian in this manner is to enable an approximation to be introduced which keeps the dimension of the Hilbert space roughly constant as sites are added. During each iteration a proportion of the basis states must be thrown away according to some systematic method. This is necessary to keep the calculation to a computationally manageable size. Within the tight-binding framework it is the only approximation in our method.

There are several possible schemes which could be used. A criterion is required that produces the smallest error on the next iteration ground state as it is the prop-

erties of the ground state which are of interest. Naïvely, the lowest energy states could be kept. More sophisticated approaches would determine which states make the largest contribution to the next iteration ground state. Whichever method is adopted, some justification will be required as will the determination of the limits of its accuracy.

The simplest method to implement is to throw away the states of highest energy, so this will be adopted initially. The diagonalization routines automatically sort eigenstates according to their eigenenergies making the procedure relatively straightforward. Thus during each step, after diagonalization but before extending the chain, the highest energy states are discarded. This is achieved by setting an energy cutoff halfway between the M th and $(M+1)$ th eigenvalue with the same occupation number as the system ground state. This is demonstrated in fig. 2. Then all states with energy higher than the cutoff are removed. The value of M can be changed to control the accuracy where higher accuracy of course entails larger processing time and memory requirements.

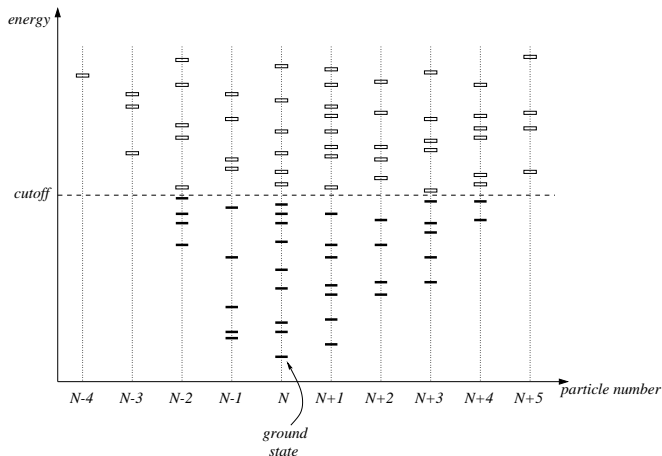


FIG. 2: This diagram illustrates the simple energy cutoff procedure for reducing the Hilbert space. It shows an example of basis states scattered according to energy and particle number. Firstly, the ground state is located. Then the excited states with the same occupation number are counted in order to set the cutoff energy as the midpoint between the M th and $(M + 1)$ th state (in this case $M = 9$). All states below the cutoff are kept and the rest are discarded.

C. Measuring the Localization Length

The aim of this new method is to understand the effect of varying system parameters, in particular the interaction strength U , on electron localization. For non-interacting systems and assuming the wavefunction has an exponentially decaying envelope, the degree of localization can be characterized by the localization length λ . This quantity is related to the transport and conductivity of the system.

In the non-interacting case a number of methods have been implemented for extracting the localization length¹². However, most methods of gauging localization cannot be simply carried across into the many-body case. The sensitivity to boundary conditions (BCs)^{12,13} does not suffer from this problem.

This method works by bringing the ends of the chain together to form a ring, which is equivalent to changing the boundary conditions from open to periodic. In fact, in so doing it is possible to introduce a complex phase factor. The essence of the method is to calculate the change in ground state energy as the boundary conditions are twisted, i.e. as the phase factor is varied. For a localized state very little change should be observed as the wave amplitude has decayed to zero. However, an extended state should experience a substantial change since the wave amplitude has not decayed off.

The simplest way to implement this approach is to use the *phase sensitivity* D . This is defined as the difference in ground state energy E_0 between the system with periodic BCs and the system with anti-periodic BCs:

$$D = E_0(\text{periodic}) - E_0(\text{anti-periodic}). \quad (5)$$

The length dependence of the phase sensitivity can be used to define λ :

$$D \propto e^{-\frac{L}{\lambda}}. \quad (6)$$

As the new recursive method works by extending a chain with open boundary conditions, it was necessary to implement the phase sensitivity perturbatively. This was done both as an analytical perturbation and as a numerical perturbation. The former actually reduces to calculating certain elements of the density matrix.

1. Analytical Perturbation

To implement the phase sensitivity as an analytical perturbation, consider the first order energy shift of the ground state $|\Phi_0\rangle$

$$\delta E_0 = \langle \Phi_0 | \delta \hat{H} | \Phi_0 \rangle, \quad (7)$$

where $\delta \hat{H} = \pm V(\hat{c}_1^\dagger \hat{c}_L + \hat{c}_L^\dagger \hat{c}_1) + U(\hat{c}_1^\dagger \hat{c}_1)(\hat{c}_L^\dagger \hat{c}_L)$ contains the hopping and interaction terms now connecting the two ends of the chain. Calculating the effect of $\delta \hat{H}$ motivates adding sites simultaneously to both ends of the chain. Given that $|\Phi_0\rangle$ is a linear combination of basis states (see eqn. 3), the effect of $\delta \hat{H}$ on $|\Phi_0\rangle$ is

$$\begin{aligned} \delta \hat{H} |\Phi_0^{L,N}\rangle = & \\ & \pm V(-1)^{s_{L-1}} \sum_j \left\{ b_{0j} |0\Phi_j^{L-2,N-1}\rangle \right. \\ & \left. + c_{0j} |1\Phi_j^{L-2,N-1}\rangle \right\} \\ & + U \sum_k d_{0k} |1\Phi_k^{L-2,N-2}\rangle. \end{aligned} \quad (8)$$

where $(-1)^{s_{L-1}}$ is a phase factor due to electron anti-symmetry arising out of the occupancy of the inner $L - 2$ sites. Substituting this into the expression for δE_0 gives

$$\delta E_0 = \pm 2V(-1)^{s_{L-1}} \sum_j b_{0j} c_{0j} + U \sum_k (d_{0k})^2. \quad (9)$$

The phase sensitivity is the difference between periodic and anti-periodic energy shifts, thus the last interaction term cancels yielding

$$D = 4V(-1)^{s_{L-1}} \sum_j b_{0j} c_{0j}. \quad (10)$$

The information required to calculate the factor $(-1)^{s_{L-1}}$ is unavailable. Fortunately the degree of localization can be calculated by using D^2 instead. Alternatively, this problem can also be avoided by choosing a different order for applying creation operators.

The “scalar product” quantity in the expression for D corresponds to calculating the off-diagonal element of the reduced density matrix,

$$\rho_{\langle 1 \dots 0 |, | 0 \dots 1 \rangle} = \rho_{\langle 0 \dots 1 |, | 1 \dots 0 \rangle} = \sum_j b_{0j} c_{0j}. \quad (11)$$

This is intuitively unsurprising because the quantity of interest is the probability that given an electron is placed at one end of the chain, *an* electron comes out the other end. Furthermore, only information about the ends of the chain is available (and required), so a *reduced* density matrix is used that sums over the redundant middle part of the chain.

2. Numerical Perturbation

The second way the phase sensitivity to boundary conditions was implemented uses a numerical perturbation. That is, the calculation proceeds as normal with open boundary conditions. At each step, working with the normal basis states two additional Hamiltonians are formed corresponding to periodic and anti-periodic BCs. These are then solved and the ground state for each type of BC is found. The phase sensitivity is then easily calculated. The basis states generated by the *open* BC Hamiltonian are kept as normal, but the states from the other two BCs are discarded.

Using this approach means performing extra diagonalizations, so it is computationally time consuming. Hence it was used to numerically verify the legitimacy of the analytical perturbation (i.e. the off-diagonal element of the reduced density matrix).

The Hamiltonian for (anti-)periodic BCs is identical to the open BCs Hamiltonian (IIB 2) but with a few extra terms. These additional terms are those calculated in the analytical perturbation for each basis state (8) and appear in the diagonal matrix elements of the Hamiltonians.

D. Model Properties

The Hamiltonian models used with this new method possess some shared properties. These will be defined in this section, again in terms of the single chain model, and suggest some consistency tests which can be used to provide limited justification for the method.

1. Definition of Energy Gaps

Several definitions of the energy gap exist in many-body systems. The numerical method under development works within the grand canonical (GC) framework so eigenvalues are grand canonical energies. Thus to convert to canonical (C) energies the following relation must be used

$$E^{GC}(N) = E^C(N) - N\mu. \quad (12)$$

Various energy gaps are defined in (13)

$$\Delta E_{\text{ph}} = E_1(N) - E_0(N) \quad (13a)$$

$$\Delta E_+ = E_0(N+1) - E_0(N) \quad (13b)$$

$$\Delta E_- = E_0(N) - E_0(N-1) \quad (13c)$$

$$\Delta E = E_0(N+1) + E_0(N-1) - 2E_0(N). \quad (13d)$$

where ΔE_{ph} (13a) is the difference between the ground state and the 1st excited state, ΔE_+ and ΔE_- (13b & 13c) are the energies to add or remove an electron from the system, and ΔE is the difference of ΔE_+ and ΔE_- (13d). When transferring to canonical energies, ΔE_+ and ΔE_- will shift by a constant $\mp\mu$. The non-interacting limit yields some predictions which simulations should reproduce.

2. Length Dependence

In the single body case there is one state per site and the bandwidth is constant so the density of states is proportional to the number of sites L . This means on average $\Delta E_{\text{ph}} \propto \frac{1}{L}$ at the same position within the band. The canonical and grand canonical versions are identical as ΔE_{ph} is a difference between states with identical particle number.

The *canonical* energy required to add a particle should be a little larger than the chemical potential. In the ground state, the highest occupied state will be the first state below the chemical potential. In order to add a particle the energy of the first state above the chemical potential is required. Thus the canonical energy is the chemical potential plus a contribution with a length dependence of $\frac{1}{L}$. The maximum of this contribution is ΔE_{ph} corresponding to the case in which, before adding the electron, the highest occupied state energy was precisely the chemical potential energy. When transferring into the grand canonical scheme ΔE_+ reduces to the $\propto \frac{1}{L}$ contribution. In the middle of the band, where $\mu = 0$, the canonical and grand canonical energies are identical.

3. Consistency Test

The energy gap definitions also give a consistency test that works in the presence of disorder, but unfortunately does not work in the presence of Coulomb interactions. Consider the energy change when one electron is added to the ground state. It can readily be seen that a relation can be found for the difference between ground state energy of the system $E_0(N)$ and the ground state with an additional particle $E_0(N+1)$

$$E_0(N+1) - E_0(N) = E_1(N) - E_0(N-1), \quad (14)$$

where $E_1(N)$ is the first excited state with the same particle number as the system ground state. Figure 3 shows the four states referred to in the relation. The right-hand

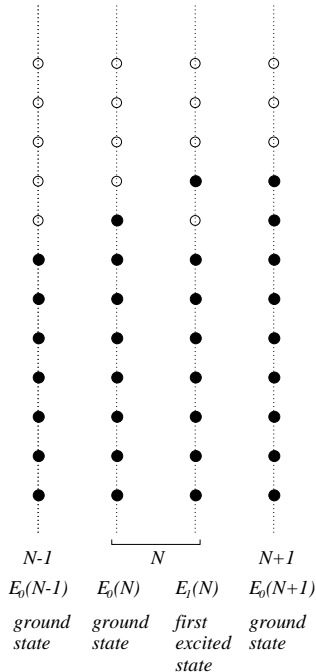


FIG. 3: Illustrates the consistency test relation between ground state energies. The filled dots are occupied single particle states.

side can be substituted into the definition of ΔE , then after canceling ΔE reduces to ΔE_{ph} . Therefore the above relation is equivalent to

$$\Delta E = \Delta E_{ph}. \quad (15)$$

The accuracy to which these equivalence relations will be satisfied depends on the number of basis states retained in each generation. If all states are kept this should be an exact formula.

4. Particle-Hole Symmetry

When a band is nearly full it is often more instructive to consider the system in terms of holes rather than particles. Even in the case with disorder and interactions there should be a symmetry between the behavior of holes in the top of the band and the behavior of electrons in the bottom of the band. The symmetry relation between the two can be found by rewriting the Hamiltonian in terms of holes and then comparing with the original electron Hamiltonian.

The Hamiltonian for the system given in terms of electron occupancy is (for open boundary conditions):

$$\hat{H} = \sum_{i=1}^L \hat{c}_i^\dagger \hat{c}_i \varepsilon_i + V \sum_{i=1}^{L-1} (\hat{c}_i^\dagger \hat{c}_{i+1} + \hat{c}_{i+1}^\dagger \hat{c}_i) + U \sum_{i=1}^{L-1} (\hat{c}_i^\dagger \hat{c}_i)(\hat{c}_{i+1}^\dagger \hat{c}_{i+1}) - \mu \sum_{i=1}^L \hat{c}_i^\dagger \hat{c}_i. \quad (16)$$

To rewrite this for holes it is necessary to define suitable creation and annihilation operators for holes, \hat{b}_i^\dagger and \hat{b}_i , respectively. The equivalence relations to particle operators are: $\hat{b}_i^\dagger = \hat{c}_i(-1)^i$ and $\hat{b}_i = \hat{c}_i^\dagger(-1)^i$. Substituting these into the electron Hamiltonian and rearranging gives a similar form of Hamiltonian to the original

$$\begin{aligned} \hat{H} = & - \sum_{i=1}^L \hat{b}_i^\dagger \hat{b}_i \varepsilon_i + V \sum_{i=1}^{L-1} (\hat{b}_i^\dagger \hat{b}_{i+1} + \hat{b}_{i+1}^\dagger \hat{b}_i) \\ & + U \sum_{i=1}^{L-1} (\hat{b}_i^\dagger \hat{b}_i)(\hat{b}_{i+1}^\dagger \hat{b}_{i+1}) + (\mu - 2U) \sum_{i=1}^L \hat{b}_i^\dagger \hat{b}_i \\ & + \sum_{i=1}^L \varepsilon_i + (L-1)U - L\mu + U\hat{b}_1^\dagger \hat{b}_1 + U\hat{b}_L^\dagger \hat{b}_L \end{aligned} \quad (17)$$

The last two terms arise from using open boundary conditions. In order to correct for these terms, from now on the original Hamiltonian will be adjusted by adding $+\frac{U}{2}\hat{c}_1^\dagger \hat{c}_1 + \frac{U}{2}\hat{c}_L^\dagger \hat{c}_L$. In the algorithm these terms are readily introduced but must only be applied to the end sites, i.e. they must be removed when extending the chain length. Once added, the equivalent Hamiltonian in terms of holes then becomes

$$\begin{aligned} \hat{H} = & - \sum_{i=1}^L \hat{b}_i^\dagger \hat{b}_i \varepsilon_i + V \sum_{i=1}^{L-1} (\hat{b}_i^\dagger \hat{b}_{i+1} + \hat{b}_{i+1}^\dagger \hat{b}_i) \\ & + U \sum_{i=1}^{L-1} (\hat{b}_i^\dagger \hat{b}_i)(\hat{b}_{i+1}^\dagger \hat{b}_{i+1}) \\ & + \frac{U}{2}\hat{b}_1^\dagger \hat{b}_1 + \frac{U}{2}\hat{b}_L^\dagger \hat{b}_L \\ & + (\mu - 2U) \sum_{i=1}^L \hat{b}_i^\dagger \hat{b}_i + \sum_{i=1}^L \varepsilon_i + L(U - \mu). \end{aligned} \quad (18)$$

This symmetry means that an exact correspondence of eigenvectors is expected to be observed at the top and bottom of the band such that

$$\begin{aligned} \hat{H}(\varepsilon_i = \varepsilon'_i, \mu = -\mu', U = U') = \\ \hat{H}(\varepsilon_i = -\varepsilon'_i, \mu = \mu' + 2U', U = U') \\ + \sum_{i=1}^L \varepsilon'_i + L(U' + \mu'), \end{aligned} \quad (19)$$

with a shift of eigenenergies according to the last two terms. In fact, the $+\sum_{i=1}^L \varepsilon'_i + L(U' + \mu')$ terms represent the energy of the full electron band which can be easily seen from the electron Hamiltonian. The significance is that the hole picture starts from the top of the band and works downward.

Moreover, because the eigenvectors are identical, the reduced density matrix method for calculating localization length will give exactly the same results either top or bottom of the band. This is because $\rho_{\langle 0 \dots 1, | 1 \dots 0 \rangle} \equiv \rho_{\langle 1 \dots 0, | 0 \dots 1 \rangle}$ from eqn. 11, and so can be used as a consistency test.

This symmetry may be extended from a single sample to the average case by noting that the probability distribution for ε_i is a symmetric function about the origin. This has two implications. Firstly, the $\sum_{i=1}^L \varepsilon_i$ term will tend to zero as the number of sites is increased. And secondly, the sign of the $-\sum_{i=1}^L \hat{b}_i^\dagger \hat{b}_i \varepsilon_i$ term can be flipped. This simplifies the equivalence relation to

$$\hat{H}(\mu = -\mu', U = U') = \hat{H}(\mu = \mu' + 2U', U = U') + L(U' + \mu'). \quad (20)$$

for an ensemble average.

The particle-hole symmetry also gives the condition for half-filling: $\mu' = U'$. This can be seen by setting $-\mu' = \mu' + 2U'$, so that in both eqns. 19 and 20 the same value for μ is specified.

E. Computational Implementation

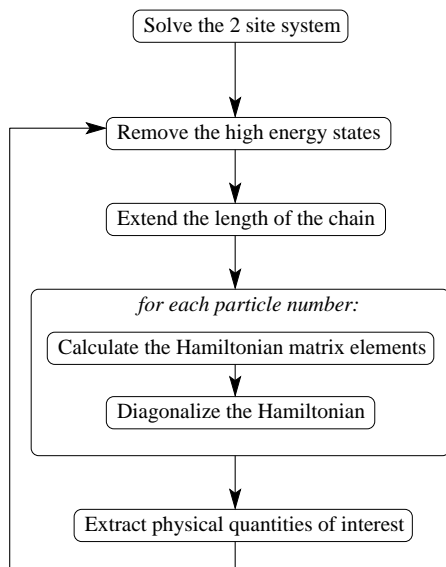


FIG. 4: A flow diagram showing the central procedure of the algorithm. This whole procedure is repeated many times with different disorder realizations.

The simulation was written in C++, making use of the object orientated facilities. Because states need to be added and removed from a set of states it was natural to use linked lists, with each link holding data for one state and the entire list representing a set of basis states or eigenstates. This results in making the code for the central algorithm less cumbersome. The structure of the central algorithm is shown in fig. 4.

To extract sensible data localization quantities must be averaged over many systems. Conventional practice is to perform a geometric average which is achieved by averaging the logarithm of the phase sensitivity. Then least-square fits were carried out to extract the localization length over a minimum of 10 sites. In addition

other quantities were recorded such as the particle density, ground state energy and energy gaps.

1. Removing States

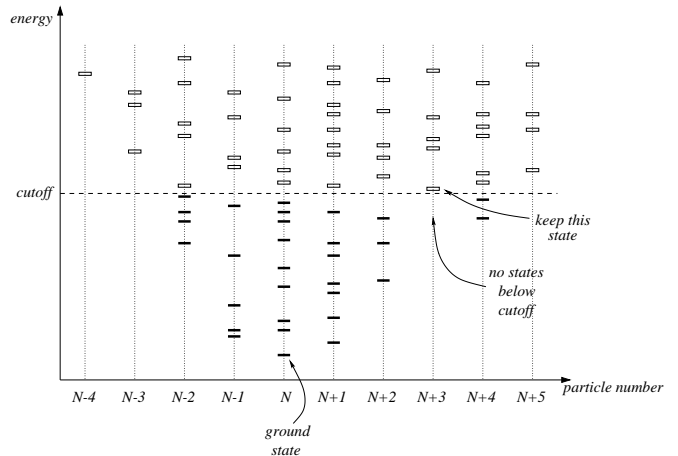


FIG. 5: This diagram illustrates how the simple energy cutoff scheme may occasionally cause difficulties. All states with $N+3$ particles will be removed, however some states with $N+4$ particles will be retained. To avoid considerable overhead in coding, the lowest energy state for $N+3$ will be kept.

One minor modification to the above procedure was made. It is simplest to code this new numerical method assuming that states exist for every particle number between two limits (in a range roughly centered around the ground state particle density). For example in fig. 2, after the Hilbert space reduction, each value of N between $N-2$ and $N+4$ inclusive have states remaining. With the reduction scheme outlined above a scenario occasionally arises whereby this assumption would be rendered invalid. Figure 5 demonstrates that it is possible for one value of N , in the fig. $N+3$, to have all states removed yet neighboring particle numbers to have states left. To cater for this rare event the code would become unnecessarily complicated. The problem can be easily overcome in such cases by retaining the lowest state even though it is above the energy cutoff.

In addition to this, the ground states corresponding to $N+1$ and $N-1$ particle numbers were always retained at each iteration. This ensures the various energy gaps can be calculated even in the rare event when the $N-1$ or $N+1$ ground state lies above the cutoff energy.

III. THE SINGLE CHAIN MODEL

This method was first applied to the Hamiltonian (1) plus the two correction terms to ensure particle-hole sym-

metry:

$$\begin{aligned} \hat{H} = & \sum_{i=1}^L \hat{c}_i^\dagger \hat{c}_i \varepsilon_i + V \sum_{i=1}^{L-1} (\hat{c}_i^\dagger \hat{c}_{i+1} + \hat{c}_{i+1}^\dagger \hat{c}_i) \\ & + U \sum_{i=1}^{L-1} (\hat{c}_i^\dagger \hat{c}_i)(\hat{c}_{i+1}^\dagger \hat{c}_{i+1}) + \frac{U}{2} \hat{c}_1^\dagger \hat{c}_1 + \frac{U}{2} \hat{c}_L^\dagger \hat{c}_L \\ & - \mu \sum_{i=1}^L \hat{c}_i^\dagger \hat{c}_i. \end{aligned} \quad (21)$$

This is the conventional 1D Anderson model with nearest neighbor interactions. In this paper hopping will always be set to $V = 1$ (hence defining the energy scale for both U and W). The following two subsections outline some useful features already known about this model in two limits: no interactions ($U = 0$) and no disorder ($W = 0$).

A. Non-Interacting Behavior

A single chain with one orbital per site has one band centered on zero with bandwidth $4V$. Including disorder will blur the edges, effectively widening the band. The localization properties of a one-dimensional non-interacting chain are well established. For any amount of disorder all eigenstates are localized. The dependence of localization length on disorder is usually quoted as¹²

$$\lambda^{-1} = \frac{W^2}{24(4V^2 - \mu^2)}. \quad (22)$$

This is only valid for small disorder. Note that the localization length diverges in the clean limit. Therefore, an important test for the new recursive method is to reproduce this behavior. However, care is required in making the correct comparison: how does this dependence carry across from the single-particle case to the many-particle case? A simple test program was constructed using exact diagonalization to calculate the phase sensitivity to boundary conditions for both the single state in the center of the band and the phase sensitivity for the grand canonical energy. Good agreement was found.

B. Clean Phase Space

The second limit to be outlined is the zero disorder phase space. This is understood because without randomness the present model can be mapped to a XXZ spin chain model and solved exactly for half-filling^{14,15,16,17}.

A program was constructed to perform exact diagonalizations on short chains in order to compare results. This was necessary because the method under development doesn't use the particle occupation basis. The computational limit is about 10 sites, but nevertheless gives valuable insight into the nature of the ground state for different regions of phase space.

At half-filling there are two limiting forms of the ground state with a crossover regime. For large repulsive interactions a charge density wave (CDW) is observed (i.e. alternate sites are occupied). For attractive interactions, electrons tend to cluster together. For open boundary conditions (with the correction for particle-hole symmetry) the transition region occurs between $U = -0.8$ and $U = -2$.

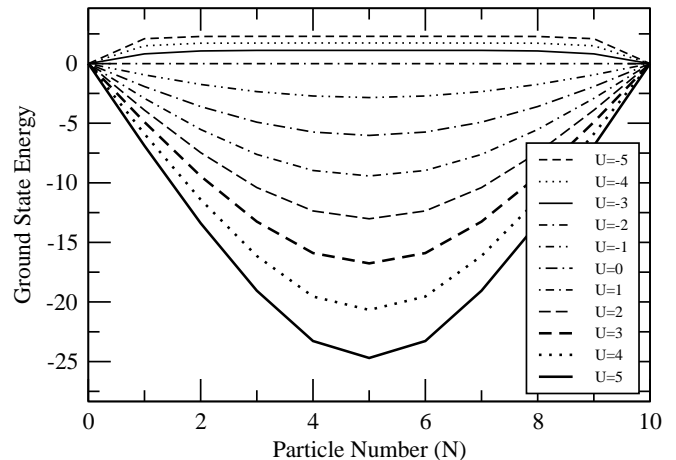


FIG. 6: Results from a (clean) short chain of 10 sites demonstrating phase separation for $U < -2$. For each particle number the ground state energy is plotted. The chemical potential is set to give half-filling as the overall ground state (i.e. $\mu = U$). Plotted energies are grand canonical.

For attractive interaction below $U = -2$, it is impossible to maintain half-filling within the grand canonical scheme. The ground state is a completely empty or completely full band (i.e. it is unstable to phase separation) as can be seen in figure 6. In fact, as the $U = -2$ limit is reached from above, the ground state energy tends toward being independent of particle number N .

In contrast, for increasing repulsive interactions, above $U = 2$ a charge gap opens up^{14,18}. In other words, the CDW above this point corresponds to a Mott insulator state. For short chains it is not possible to pinpoint where this gap begins.

C. Previous Work

Perhaps the most substantial work is that of Giamarchi and Schulz¹⁹, although they acknowledge an earlier paper²⁰. For the present one-dimensional model repulsive interactions increase localization because the CDW is pinned by the disorder. In contrast, attractive interactions decrease localization. In fact, a delocalized phase is predicted for sufficiently attractive interactions. Giamarchi and Schulz develop a k -space Renormalization Group approach to study the transition. The existence of this transition is ascribed to competition between disorder and superconducting fluctuations¹⁹.

Numerical work has sought to verify these predictions and in particular to map out the delocalized regime. One paper¹⁸ performs exact diagonalizations on small systems (up to 22 sites). The results are consistent with the expected delocalized phase, although because the chain length is so small they cannot exclude the possibility that the localization length is very large.

The first DMRG study¹⁴ focused on the effect of disorder on the Mott state. The authors conclude that even weak disorder destroys the charge gap and long-range order associated with the CDW state (although the nature of elementary excitations remain unchanged).

The most extensive work has been conducted by Schmitteckert et al. applying DMRG to both the interacting Anderson model and to the related problem of persistent currents in mesoscopic rings^{7,13,21,22}. The first study examining Anderson localization¹³ was on chains extending up to 60 lattice sites. The degree of localization was measured by the phase sensitivity to boundary conditions. Two regimes were found: a localized phase, $U > -1$, and delocalized regime, $U < -1$, consistent with work already mentioned. In fact, it was found repulsive interactions increase localization. After considerable numerical effort a phase diagram was produced showing where the two regions lie in disorder-interaction space. The authors believe the earlier attempt¹⁸ based on an RG procedure over estimates the delocalized regime by a factor of 4. Other authors, Römer²³ and Schuster et al.²⁴, have mapped out an extended regime for the same model but with the Aubry-André quasi-periodic potential. However its shape in disorder-interaction phase space takes on a different form.

In two more recent papers^{7,22} Schmitteckert et al. showed that important physics is washed out in the process of ensemble averaging used in ascertaining numerical data. They examined the chaotic region between a chain characterized as an Anderson insulator and characterized as a Mott insulator corresponding to the strongly disordered and the strongly correlated limits respectively.

Schmitteckert et al. showed that in this transition region there are sharp charge reorganizations causing a dramatic increase in phase sensitivity (delocalization) of up to 4 orders of magnitude. It is important to note that the position in parameter space where these reorganizations occur is sample dependent such that on averaging over many samples only a slight delocalization effect can be observed. This is found for large disorder $W = 7, 9$ and for small *repulsive* interactions $U < V$. Typically two or three distinct charge reorganizations may occur per sample as it is moved between a Mott insulator and an Anderson insulator state. Attractive interactions favor a more inhomogeneous charge density (forming clusters) and repulsive interactions favor more homogeneous charge density (CDW) as expected. Of course, this effect will be most pronounced at half filling since for lower densities electrons can avoid each other spatially.

This phenomenon was explained further in terms of avoided level crossings²² of the ground state and first-

excited state. However, to be critical these results are based on small system sizes (20 sites) and may well be due to finite-size effects.

D. Determining Limits and Accuracy

As appropriate for any new method, the extent of its validity should be tested before producing results. There are three points which should be established:

- The program is working properly.
- The two methods for gauging the degree of localization yield consistent results.
- The approximation for eliminating basis states is controlled.

The last of these will be the most involved.

1. Determining Numerical Limits

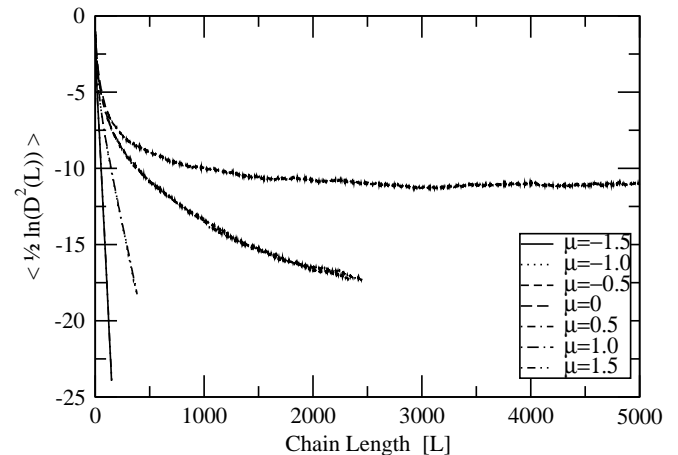


FIG. 7: The graph is a plot of the average of $\frac{1}{2} \ln(D^2)$ as a function of chain length L where D is the phase sensitivity (10). Averages are geometric, that is the mean of $\ln(D^2)$ is found. The chain length is allowed to extend until numerical precision is lost. The $\mu = 0$ case was stopped at 20,000 sites as it had saturated long before. System parameters are $W = 2$, $U = 0$ and the energy cutoff is set using $M = 10$ (corresponding to a total of approximately 160 basis states per iteration). The averages were taken over 2000 systems.

The first simulations aimed to determine the broad numerical limits of this new method. Figure 7 shows some typical results where the chain length has been allowed to extend as far as possible. A range of values of μ were used, spread across the band (between $\mu = -2$ and $\mu = 2$ in the non-interacting case). The lines pair up, with $\mu = -\mu'$ and $\mu = +\mu'$ giving near identical results and thus demonstrating the anticipated symmetry in the band.

Straight lines indicate exponential localization, which is seen near the band edge. However, in the center of the band different behavior is observed: the curves show some form of decay which saturates at large chain lengths. In fact, for the $\mu = 0$ case, the curve had clearly saturated and so was stopped at 20 000 sites.

Apart from the $\mu = 0$ case, all simulations continued until numerical precision limits were reached. This limit is encountered when calculating the phase sensitivity. Off-diagonal elements of the reduced density matrix correspond to “scalar product” type quantities (11). Using this as an analogy, when the two vectors become almost perpendicular the product becomes very small. In this limit, numerical rounding dominates over the physics rendering any results based on this regime meaningless. Arising out of this, a criterion was devised to automatically halt simulations before this numerically inaccurate region is reached. Taking up the analogy again, when the scalar product divided by the norm of the two vectors is comparable to the floating-point precision then only “noise” is being calculated. This condition gives the upper length limit for linear fits which determine the inverse localization length. A lower limit was also set in which typically the first 20% of sites were ignored to allow the simulation to “settle down”.

2. Particle-Hole Symmetry Test

The particle-hole symmetry test can be verified by looking at two chains using the same random distribution of site energies, but with one the negative of the other (see eqn. 19). On doing so identical results are obtained. Thus in the non-interacting case the electron-hole consistency test is convincingly satisfied.

Applying a small electron interaction force $U = 0.1$ causes the paired lines to split. This is also expected. Once the $+\frac{U}{2}\hat{c}_1^\dagger\hat{c}_1 + \frac{U}{2}\hat{c}_L^\dagger\hat{c}_L$ correction terms are included, the two lines then collapse on top of each other again.

3. Comparison of the two Phase Sensitivity Methods

As explained earlier in section II C, the reduced density matrix method of determining the extent of localization could be verified by calculating the phase sensitivity as a numerical perturbation. It was found that the two methods are in good agreement (fig. 8). Given the significant computational processing time required for the numerical perturbation method, normally only the reduced density matrix method will be used.

4. Reducing the Number of Basis States (Revisited)

The initial results (fig. 7) show that the method fails in the middle of the band - exponential decay is not observed in the non-interacting case. This must be due to

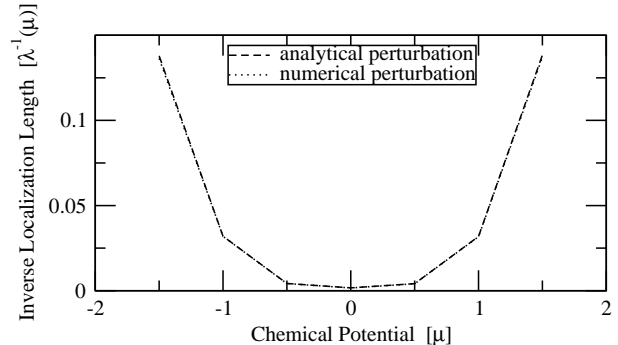


FIG. 8: This graph shows the inverse localization length (obtained from a linear fit) against a range of values of the chemical potential μ . The two lines correspond to the two methods of determining localization and they show very good agreement. System parameters are $W = 2$, $U = 0$ with chains allowed to extend to a maximum of 500 sites. The averages were taken over 2500 systems and the energy cutoff set by $M = 10$ (corresponding to a total of approximately 160 basis states per iteration). The error bars represent one standard deviation.

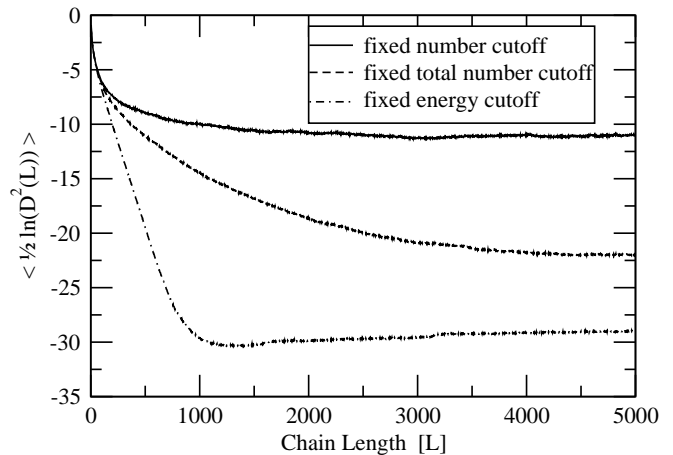


FIG. 9: The graph is a plot of the average of $\frac{1}{2} \ln(D^2)$ against chain length L . The parameters are the same as fig. 7, but restricted to the middle of the band ($\mu = 0$). The only difference between the three curves is the procedure for discarding basis states.

the Hilbert Space reduction criterion, as it is the only approximation in the method. A simple variant on the original procedure was tried: the *total* number of states for all particle numbers was fixed rather than using a fixed number for the ground state particle number only. This simple modification induced a significant change in the results. Although the decay was still non-exponential, this change clearly yields an improvement toward the expected behavior (fig. 9).

Presumably the key difference between the methods is that using states from all particle numbers results in an energy cutoff which fluctuates less. The natural criterion to try next is a fixed energy cutoff. This can be done by

averaging the value of the cutoff using the fixed number of states method. Then a fit of the cutoff as a function of chain length could be used as a fixed energy cutoff. It turns out that it is not possible to do this as an absolute cutoff because the ground state energy fluctuates too much. However it can successfully be done as a fixed energy cutoff relative to the ground state. When implemented exponential decay is observed in the middle of the band (fig. 9).

We conjecture that this dramatic improvement, resulting from an apparently innocuous change in cutoff methods, can be explained in terms of energy level statistics. Consider the middle of the band with no interactions: electrons should be localized, with states obeying Poisson statistics. One may envisage the system accidentally encountering a higher density of low lying energy states. According to the original method, the energy cutoff is correspondingly lower. Thinking in terms of *energy level repulsion*, this would result in a release of “pressure” as a larger number of states are removed. The opposite scenario in which states accidentally spread wider than average may also be considered. In this case, the cutoff has a smaller effect than normal. The combined effect is to reduce fluctuations, causing the system to bear more resemblance to a Wigner distribution. In other words the system tends toward delocalization, consistent with the data on fig. 9.

The second cutoff method implemented worked by fixing the cutoff using states across all particle numbers. According to the picture just outlined, the same effect of dampening fluctuations should still be present, although less severe because using a greater number of states reduces fluctuations of the cutoff energy. This can also be observed in figure 9, where the delocalizing effect is not so strong.

The third procedure for discarding states used a fixed energy cutoff, which is completely uncorrelated to the density of low lying states. Therefore the delocalizing effect is completely absent.

E. Comparison with Non-Interacting Results

The new fixed energy cutoff may be used to provide further verification by checking that when interactions are turned off non-interacting results can be reproduced. This is particularly important as some well established methods applied to the two-interacting particle model can fail in this respect (e.g. the Transfer Matrix Method^{25,26}).

1. Dependence on Disorder

As a test of the accuracy of the method, figure 10 was produced. The calculated results should correspond to the known result (22). The new method seems to give a dependence on W greater than W^2 . Values are at least

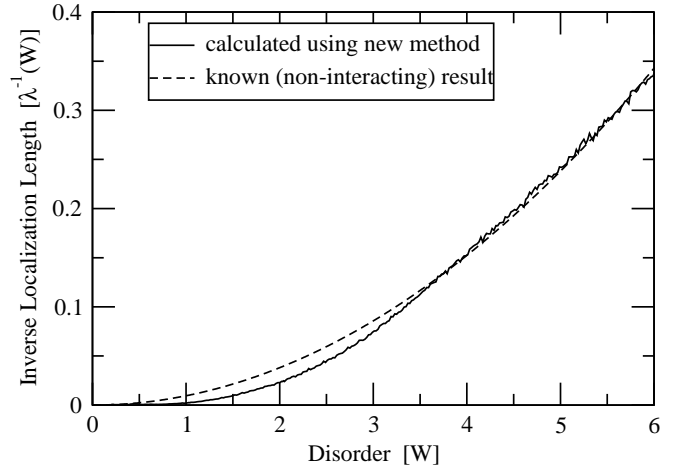


FIG. 10: Graph showing the dependence of inverse localization length upon the disorder when interactions are turned off. Results from the new method should correspond to known result for the middle of the band. Systems were allowed to extend up to 1000 sites, retaining an average of 480 basis states per iteration. Averages were taken over 1000 disorder realizations.

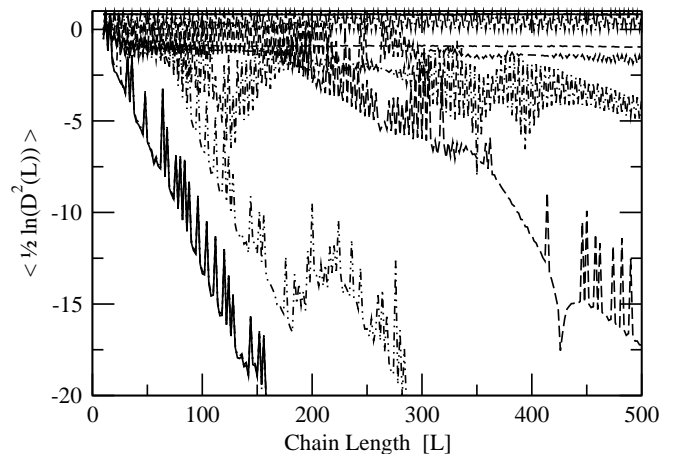


FIG. 11: Graph showing single sample results for low disorder ($W = 0.2$). The new method fails in this limit. The only difference between the lines is a slight variation in the energy cutoff.

of the correct order of magnitude. It should be noted, however, that in the clean limit and for low disorder the new method fails to produce meaningful results. Figure 11 shows a set of results corresponding to the same system but with the energy cutoff slightly varied. The change in behavior is quite dramatic and dominated by large oscillations. These effects do not occur for stronger disorder.

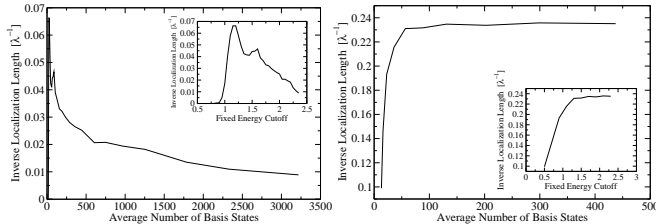


FIG. 12: Graph showing the dependence of inverse localization length on the average number of basis states retained per iteration for the non-interacting case with disorder $W = 2$ (left) and $W = 5$ (right). The insets show this quantity plotted against the actual energy cutoff used. Such plots can be used to test for convergence. Data was averaged over 100 systems with chains extending up to 1000 sites.

2. Convergence

Figure 12 is used to determine whether the method converges to the known value of the localization length in the middle of the band. For $W = 2$, eqn. 22 implies $\lambda^{-1} \approx 0.038$. Hence for the calculation using the largest matrices the localization length is over estimated by about a factor of 4. As anticipated from fig. 10, convergence is much better for $W = 5$. In this case, eqn. 22 gives $\lambda^{-1} \approx 0.24$. Figure 12 shows the new method converging at a value close to this result. One could consider proceeding by just examining interaction effects for $W > 4$. However, interesting physics is expected when disorder and interactions are of similar strength. Note that the standard deviation, $W/\sqrt{12}$, is a more satisfactory measure of disorder, so that this condition is fulfilled when $W = \sqrt{12}$ and $U = \pm 1$.

3. Energy Gaps

Earlier, in section IID 1 it was noted that in the non-interacting limit there is a relation between two of the energy gap definitions (15). This condition was found to be obeyed provided a large proportion of basis states were retained (i.e. only possible for short chain lengths).

Also in this limit, the energy gaps should have a specific dependence on length. This is rigorously known in the clean limit as $\propto \frac{1}{L}$ for ΔE , ΔE_{ph} and ΔE_+ . In fact, when averaged, systems with disorder exhibit the same behavior. Figure 13 shows how results from the new method compares with the non-interacting results. In both cases the decay was only satisfactorily observed for short chain lengths. The charge gap decays to a value above zero. The oscillations arise due to the removal of states which can be established by varying the number of states retained. This saturation and oscillatory behavior was also observed for the other two gap definitions.

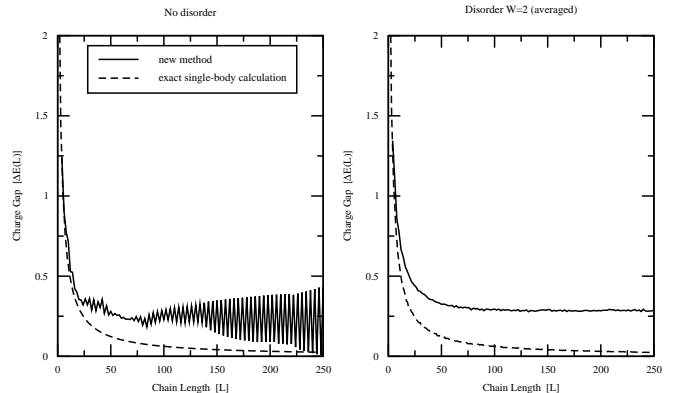


FIG. 13: Graphs showing the dependence of the charge gap ΔE on chain length. The black lines are results from the new method under development and for comparison the 2nd line represents exact results from a single-body calculation. The left-hand side shows the clean case and the right-hand side is the average over 1000 systems with disorder $W = 2$. The new fixed energy cutoff was used to remove basis states (with an average of 700 per iteration).

IV. RESULTS

Despite the unanswered questions, results were successfully obtained using the *fixed energy* cutoff procedure for eliminating states. The value for the cutoff was determined by first using the fixed number procedure for a small number of systems. When the average number of basis states is given, it refers to the number of basis states used with the fixed number procedure in order to determine the fixed energy cutoff. In addition note that previous work by other authors focuses on the case of half-filling, so results presented in this section also examine this particle density.

A. Dependence on Interaction Strength

Of central interest is the effect of electron-electron interactions on localization. Figure 14 shows the calculated dependency for disorder $W = 2$. Three different energy cutoffs were used corresponding to different numbers of retained states.

The overall behavior is unambiguous: repulsive interactions enhance the effect of disorder whereas attractive interactions reduce it. For $U > 0$ the inverse localization length has an approximately linear relationship to interaction strength. Below $U = -1$ the localization length diverges. This apparently extended regime is anticipated from previous work (section III C).

Note that due to the “flattening” effect (fig. 6) toward the phase separation the many-body density of states rises rapidly with energy. For a fixed energy cutoff this means that more states are retained over a greater range of particle numbers. This reduces computational performance and so the region $-2 < U < -1.8$ has not been

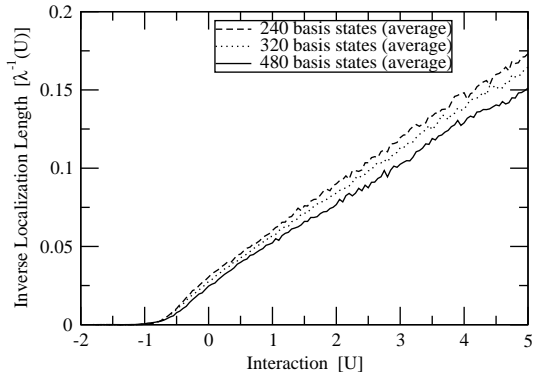


FIG. 14: The dependence of localization length on interaction strength. The three lines correspond to different energy cutoff values. Each line is averaged over 1000 systems which are allowed to extend to a maximum of 1000 lattice sites. Disorder $W = 2$.

explored. Data was obtained down to about $U = -1.8$ and is displayed in fig. 14.

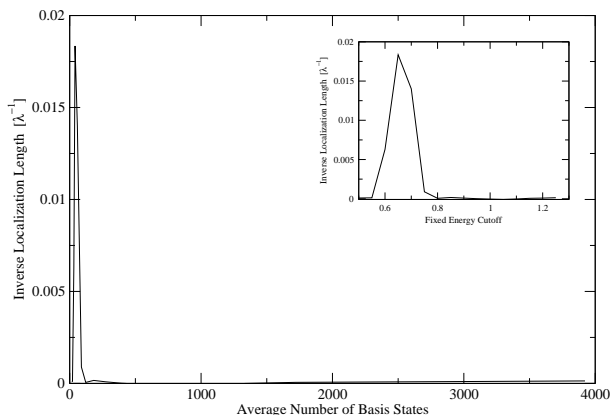


FIG. 15: Graph showing the dependence of inverse localization length on the average number of retained basis states in order to test convergence in the delocalized regime. The value of interaction strength chosen was $U = -1.4$. The inset shows the dependence on the fixed cutoff energy. The data is averaged over 100 systems with chains allowed to extend to a maximum of 1000 sites. Disorder $W = 2$.

To explore the convergence, one point in the middle of the delocalized regime was chosen and its convergence properties were explored. Figure 15 demonstrates that, within the computational limits, the extended regime is robust.

B. Disorder-Interaction Phase Space

Having confirmed the existence of a delocalized regime for attractive interactions, it was natural to attempt to map out the extent of this region. This was done in disorder-interaction phase space as plotted in fig 16. The area marked as delocalized corresponds to systems with a

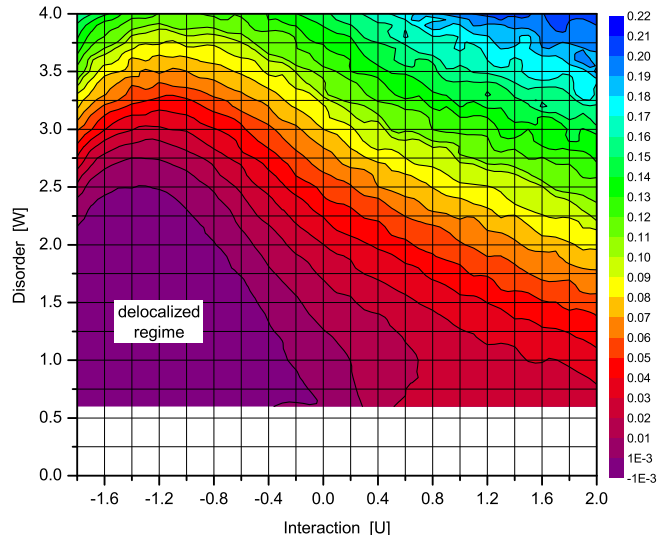


FIG. 16: Disorder-interaction phase space plot for the single chain model at half-filling. The spectrum represents the degree of localization. The lowest interval corresponds to a localization length greater than 1000 sites. This contour plot was produced using over 1300 points. Each point was averaged over 250 systems in which chains were allowed to extend to 2000 sites and approximately 240 basis states were retained per iteration. Data for $W < 0.6$ is not shown because the method is unreliable for low disorder as discussed earlier.

localization length greater than 1000 sites. If the number of systems averaged over were increased then this criterion could be made more stringent. With this definition it can be seen that the delocalizing effect does not extend beyond $W = 2.5$. The extended region appears to cross the non-interacting line for lower disorder. However, the method is unable to produce meaningful results for low disorder. The phase sensitivity tends to be dominated by oscillations which appear as the clean limit is approached (see fig.11). The (unreliable) results which were obtained indicate that the proximity of the delocalization in fact decreases for lower disorder. Hence this remains an open question.

C. Determination of Exponents

It is tempting to describe the change from a localized system to a delocalized system in the language of second-order phase transitions. Although, there is no *a priori* reason for believing the transition can be described in this way, it is clear that a description as a first-order transition is ruled out by the absence of any discontinuities. Working on this assumption, the obvious quantity to calculate is the exponent defined as

$$\lambda^{-1} = A(U - U_c)^\nu \quad U > U_c, \quad (23)$$

where A is a coefficient, ν is the exponent and U_c is the critical interaction strength where the transition occurs.

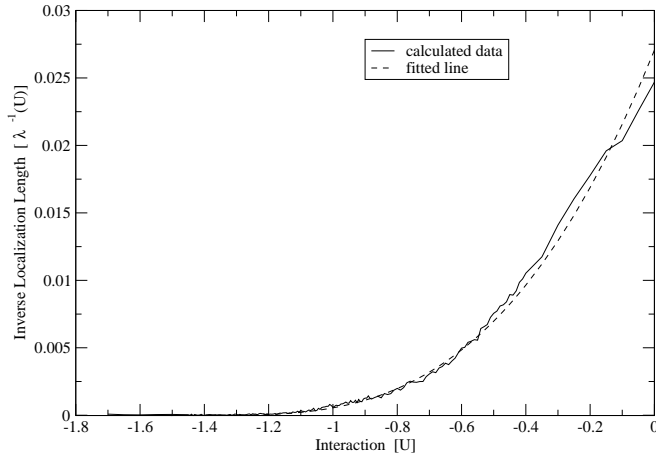


FIG. 17: This graph is the same as the black line in fig. 14 but focusing on the transition region. The fitted line corresponds to $U_c = -1.375$ and $\nu = 3.0$ and shows good agreement.

Two factors make determining this exponent difficult: Firstly, data can only be used on one side of the transition. Secondly, the precise value of U_c is unknown and no scaling analysis is available. Consequently, fitting the data shown on fig. 14 using a log-log plot proved unsatisfactory. Likewise, attempting to fit all 3 parameters (A , U_c and ν) simultaneously was also uncontrolled. Therefore, an estimate for the critical interaction strength was visually estimated and then the other two parameters could be fitted. Although, this procedure is less than ideal, it appeared to be the most satisfactory approach. The estimated range for U_c is $-1.45 \leq U_c \leq -1.3$. Using a number of values within this range the two other parameters (A and ν) were fitted, giving $\nu \approx 3.0 \pm 0.4$. This exponent has been plotted with the central value of U_c on fig. 17. The fit is not perfect, the deviation may either reflect the absence of a known scaling analysis or that the assumption of a second-order phase transition is incorrect.

However, it is at least clear that away from the transition there is an approximately linear relationship between

inverse localization length and the interaction strength. Further, by inspecting fig. 14, the exponent must therefore be greater than 1 in the vicinity of the transition. The determined value for ν is consistent with that observation.

It would be desirable to perform a similar procedure for other values of disorder and to determine the disorder exponent at a fixed interaction strength (i.e. approaching the transition from above on fig. 16). However, the quality of data presently obtained is inadequate. Schmitteckert et al.¹³, argue that the exponent is non-universal.

D. Summary

We have presented a method of studying disordered and interacting quasi-1-dimensional systems which combines aspects of the transfer matrix and DMRG approaches. While the method works well and is able to study significantly larger systems than have been achieved hitherto, there is still room for improvement. In particular the strategy for reducing the Hilbert space and compensating for the side effects of the reduction is still too simplistic. It would be useful to understand why the method fails so dramatically for low disorder. Nevertheless the method is generalizable to more complex problems such as the Hubbard model or strips of finite width. It could eventually be possible to combine such an approach with finite size scaling in order to study the metal-insulator transition.

As a first application of our method we have presented results on spinless fermions in 1D. There is qualitative agreement with previous work: repulsive interactions increase the effect of disorder and attractive interactions have the opposite effect. We have mapped out the delocalized regime and found some disagreement with previous work. According to our results, DMRG studies *under* estimate this region by a factor of 2 and an earlier study *over* estimates it by a factor of 2. We have also made a first estimate of the critical exponent of this transition, but our data is not yet sufficient to test its universality.

* Electronic address: a.mackinnon@imperial.ac.uk

¹ K. Slevin and T. Ohtsuki, Phys. Rev. Lett. **82**, 382 (1999).

² S. Kravchenko, G. Kravchenko, J. Furneaux, V. Pudalov, and M. d'Iorio, Phys. Rev. B **50**, 8039 (1994).

³ D. Shepelyansky, Phys. Rev. Lett. **73**, 2607 (1994).

⁴ M. Ortuño and E. Cuevas, Europhys. Lett. **46**, 224 (1999).

⁵ S. White, Phys. Rev. Lett. **69**, 2863 (1992).

⁶ S. White, Phys. Rev. **B48**, 10345 (1993).

⁷ P. Schmitteckert, R. Jalabert, D. Weinmann, and J.-L. Pichard, Phys. Rev. Lett. **81**, 2308 (1998).

⁸ P. Schmitteckert, T. Schulze, C. Schuster, P. Schwab, and U. Eckern, Phys. Rev. Lett. **80**, 560 (1998).

⁹ A. MacKinnon and B. Kramer, Phys. Rev. Lett. **47**, 1546 (1981).

¹⁰ A. MacKinnon and B. Kramer, Z. Phys. **B51**, 1 (1983).

¹¹ P. Anderson, Phys. Rev. **109**, 1492 (1958).

¹² B. Kramer and A. MacKinnon, Rep. Prog. Phys. **56**, 1469 (1993).

¹³ P. Schmitteckert, T. Schulze, C. Schuster, P. Schwab, and U. Eckern, Phys. Rev. Lett. **80**, 560 (1998).

¹⁴ H. Pang, S. Liang, and J. Annett, Phys. Rev. Lett. **71**, 4377 (1993).

¹⁵ C. Yang and C. Yang, Phys. Rev. **150**, 321 (1966).

¹⁶ C. Yang and C. Yang, Phys. Rev. **150**, 327 (1966).

¹⁷ C. Yang and C. Yang, Phys. Rev. **151**, 258 (1966).

¹⁸ G. Bouzerar and D. Poilblanc, J. Phys. I France **4**, 1699 (1994).

¹⁹ T. Giamarchi and H. Schulz, Phys. Rev. B **37**, 325 (1988).

- ²⁰ W. Apel and T. Rice, Phys. Rev. B **26**, 7063 (1982).
- ²¹ P. Schmitteckert and U. Eckern, Phys. Rev. B **53**, 15397 (1996).
- ²² D. Weinmann, P. Schmitteckert, R. Jalabert, and J.-L. Pichard, Eur. Phys. J. B. **19**, 139 (2001).
- ²³ C. Schuster, R. Römer, and M. Schreiber, Phys. Rev. B **65**, 115114 (2002).
- ²⁴ A. Eilmes, R. Römer, C. Schuster, and M. Schreiber, *Two and more interacting particles at a metal-insulator transition* (2001), cond-mat/0102251.
- ²⁵ R. Römer and M. Schreiber, Phys. Rev. Lett. **78**, 515 (1997).
- ²⁶ M. Leadbeater, R. Römer, and M. Schreiber, Eur. Phys. Jour. B **8**, 643 (1999).